Molecular Pharmacology Fast Forward. Published on April 8, 2014 as doi: 10.1124/mol.113.091322
This article has not been copyedited and formatted. The final version may differ from this version.

Title page:

The 19S deubiquitinase inhibitor b-AP15 is enriched in cells and elicits rapid commitment to cell death

Xin Wang, William Stafford, Magdalena Mazurkiewicz, Mårten Fryknäs, Slavica Brjnic, Xiaonan Zhang, Joachim Gullbo, Rolf Larsson, Elias Arnér, Padraig D'Arcy and Stig Linder

Cancer Center Karolinska, Department of Oncology and Pathology, Karolinska Institute, SE-171 76 Stockholm (X.W, M.M., S.B., X.Z., P.D., S.L.), Department of Medical Sciences, Division of Clinical Pharmacology, Uppsala University, SE-751 85 Uppsala (M.F., J.G., R.L., S.L.), Division of Biochemistry, Department of Medical Biochemistry and Biophysics, Karolinska Institutet, Stockholm SE-171 77, Sweden (W.S., E.A.).

Molecular Pharmacology Fast Forward. Published on April 8, 2014 as DOI: 10.1124/mol.113.091322
This article has not been copyedited and formatted. The final version may differ from this version.

Running title page:

Running title: Commitment to apoptosis by a 19S deubiquitinase inhibitor

Corresponding author: Stig Linder, Cancer Center Karolinska, Department of Oncology and Pathology, Karolinska Institute, SE-171 76 Stockholm; phone: +46-8-51772452; fax: +46-8-339031; e-mail Stig.Linder@ki.se

Document statistics:

Number of text pages: 40 (Abstract, Introduction, M & M, Results and Discussion: 25)
Number of tables: 1
Number of figures: 7
Number of supplementary figures: 4
Number of references: 48
Numbers of words in Abstract: 234
Numbers of words in Introduction: 696
Numbers of words in Discussion: 1308

Abbreviations: 12δ-PGJ2, 12δ-prostaglandin J2; 19S RP, 19S regulatory particle; 20S CP, 20S core particle; AMC, 7-amino-4-methylcoumarin; Bcl-2, B-cell lymphoma 2; CrEL, Cremophor EL; DNTB, 5,5'-dithiobis-2-nitrobenzoic acid; EGFP, enhanced green fluorescent protein; FDA, fluorescein diacetate; FMCA, fluorometric microculture cytotoxicity assay; GR, glutathione reductase; GSSG, glutathione disulfide; Hmox-1, heme oxygenase (decycling) 1); K18, keratin 18; MTT, 3-(4,5-dimethylthiazol-2-yl)-2,5-diphenyltetrazolium bromide; PARP, Poly (ADP-ribose) polymerase; PVDF, polyvinylidene difluoride; Rpn11/POH1, regulatory particle subunit 11/pad one homolog-1; SI, survival index; TrxR, thioredoxin reductase; TUNEL, terminal deoxynucleotidyl transferase dUTP nick end labeling; Ub-VS, ubiquitin vinyl sulphone; UCHL5, ubiquitin carboxyl-terminal hydrolase L5; UPS, ubiquitin proteasome system; USP14, ubiquitin specific peptidase 14; YFP, yellow fluorescent protein.

Molecular Pharmacology Fast Forward. Published on April 8, 2014 as DOI: 10.1124/mol.113.091322
This article has not been copyedited and formatted. The final version may differ from this version.

ABSTRACT

b-AP15 is a small molecule inhibitor of the USP14/UCHL5 deubiquitinases of the 19S proteasome which shows anti-tumor activity in a number of tumor models, including multiple myeloma. b-AP15 contains an α, β-unsaturated carbonyl unit which is likely to react with intracellular nucleophiles such as cysteine thiolates by Michael addition. We found that binding of b-AP15 to USP14 is partially reversible, and that inhibition of proteasome function is reversible in cells. Despite reversible binding, tumor cells are rapidly committed to apoptosis/cell death after exposure to b-AP15. We show that b-AP15 is rapidly taken up from the medium and enriched in cells. Enrichment provides an explanation to the stronger potency of the compound in cellular assays compared to *in vitro* biochemical assays. Cellular uptake was impaired by 30 min pre-treatment of cells with low concentrations of N-ethylmaleimide (10 μM), suggesting that enrichment was thiol dependent. We report that in addition to inhibition of deubiquitinases, b-AP15 inhibits the selenoprotein thioredoxin reductase (TrxR). Whereas proteasome inhibition was closely associated with cell death induction, inhibition of TrxR was not. TrxR inhibition is, however, likely to contribute to triggering of oxidative stress observed with b-AP15. Furthermore, we present structure-activity, *in vivo* pharmacokinetic and hepatocyte metabolism data for b-AP15. We conclude that the strong enrichment of b-AP15 in cells and a rapid commitment to apoptosis/cell death are factors that are likely to contribute to the strong anti-tumor activity of this compound.

Molecular Pharmacology Fast Forward. Published on April 8, 2014 as DOI: 10.1124/mol.113.091322
This article has not been copyedited and formatted. The final version may differ from this version.

Introduction

The ubiquitin proteasome system (UPS) is the major intracellular protein degradation system in eukaryotic cells (Hershko and Ciechanover, 1998). The 26S proteasome complex consists of a 20S core particle (20S CP) which is associated with one or two 19S regulatory particles (19S RP). The 19S particles bind polyubiquitin-linked polypeptides and present them to the 20S degradative units (Groll et al., 1999). The efficient degradation of ubiquitinated substrates requires both unfolding and removal of polyubiquitin chains. The latter function is mediated by specific deubiquitinases which cleave the isopeptide bonds between the C-terminal carboxyl of ubiquitin and the amino group of a lysine residue on an adjacent protein (Hershko and Ciechanover, 1998). Three different deubiquitinases are associated with 19S RPs. The USP14 and UCH37/UCHL5 enzymes cleave polyubiquitin chains from the distal ends and are suggested to promote substrate rescue rather than degradation (Lee et al., 2011). USP14 and UCHL5 are cysteine enzymes that become activated after being associated with the proteasome (Lee et al., 2011). The third deubiquitinase associated with the 19S RP is the Zn^{2+}-dependent metalloprotease Rpn11/POH1. This enzyme cleaves entire polyubiquitin chains from substrates in a process that is tightly coupled to degradation (Verma et al., 2002; Yao and Cohen, 2002).

Inhibition of the proteasome is thought to lead to a disruption of the balance of proliferative and anti-proliferative signals in the cell, leading to cell-cycle arrest and induction of apoptosis (Adams, 2001; Caravita et al., 2006; Chauhan et al., 2005). Bortezomib (PS-341, Velcade®), a dipeptidyl boronic acid, is a selective inhibitor of the 26S proteasome which has shown activity against several malignant cell types and has been approved by the FDA for the treatment of patients with multiple myeloma and mantle cell lymphoma (Caravita et al., 2006; Chauhan et al., 2005). Proteasome inhibitors have been reported to sensitize malignant cells to

Molecular Pharmacology Fast Forward. Published on April 8, 2014 as DOI: 10.1124/mol.113.091322
This article has not been copyedited and formatted. The final version may differ from this version.

standard chemotherapy and attenuate inducible resistance to standard chemotherapeutical agents (reviewed in (Voorhees and Orlowski, 2006)).

The prostaglandin D2 derivative 12δ-PGJ2 has been reported to be an inhibitor of cellular deubiquitinase activity (Mullally and Fitzpatrick, 2002; Mullally et al., 2001). This class of prostaglandins contain α, β-unsaturated carbonyl groups that can form covalent adducts with free thiols in proteins by Michael addition (Suzuki et al., 1997). A number of nonprostanoid compounds containing similar unsaturated dienones have also been reported to inhibit deubiquitinase activity (Aleo et al., 2006; D'Arcy et al., 2011; Kapuria et al., 2010; Mullally and Fitzpatrick, 2002; Zhou et al., 2013). Since the majority of cellular deubiquitinases are cysteine proteases, their inhibition by 12δ-PGJ2 and structurally related compounds are logical. However, these different compounds show various selectivities to cellular deubiquitinases (D'Arcy et al., 2011; Kapuria et al., 2010; Zhou et al., 2013). Despite sharing the same element of α, β-unsaturated carbonyl groups, 12δ-PGJ2 and AC17 are irreversible deubiquitinase inhibitors (Mullally and Fitzpatrick, 2002), whereas in contrast b-AP15 was reported to be a reversible inhibitor (D'Arcy et al., 2011).

The USP14/UCHL5 inhibitor b-AP15 inhibits proteasomal function in cells exposed to this compound. b-AP15 is preferentially cytotoxic to tumor cells and shows antitumor activity in both syngeneic and xenograft tumor models (D'Arcy et al., 2011; Tian et al., 2013). The cellular response to b-AP15 is similar, but not identical to, the proteasome inhibitors MG262 and bortezomib (Brnjic et al., 2013; D'Arcy et al., 2011). Similar to bortezomib, b-AP15 causes induction of chaperone expression and oxidative stress, but these responses are stronger in cells exposed to b-AP15 (Brnjic et al., 2013). The mechanism of the strong oxidative stress response is not known, and was speculated to be related to proteotoxicity (Brnjic et al., 2013).

b-AP15 is cytotoxic to myeloma cells that have acquired resistance to bortezomib (Tian et

Molecular Pharmacology Fast Forward. Published on April 8, 2014 as DOI: 10.1124/mol.113.091322
This article has not been copyedited and formatted. The final version may differ from this version.

al., 2013) and is a candidate for clinical drug development We here set out to characterize the molecular pharmacology of this drug. We show that b-AP15 actively is enriched in target cells and elicits an irreversible commitment to apoptosis/cell death. In addition, we provide a mechanism for the previously reported strong induction of oxidative stress by this compound (Brnjic et al., 2013) by demonstrating that b-AP15 also inhibits the activity of thioredoxin reductase (TrxR). The possible importance of this off-target activity for proteasome inhibition and cell death was investigated.

Molecular Pharmacology Fast Forward. Published on April 8, 2014 as DOI: 10.1124/mol.113.091322
This article has not been copyedited and formatted. The final version may differ from this version.

Materials and Methods

Materials. b-AP15 ((3E,5E)-3,5-bis[(4-nitrophenyl)methylidene]-1-(prop-2-enoyl)piperidin-4-one) was obtained from Oncotargeting AB (Uppsala, Sweden) and bortezomib from ApoEx (Bromma, Sweden). Compounds were dissolved in DMSO. Control cultures received the same final concentration of solvent as treated ones. Compound b-AP107 (NSC687849; (3E,5E)-3,5-bis[(4-chlorophenyl)methylidene]-1-prop-2-enoylpiperidin-4-one) and b-AP113 (NSC687853; (3E,5E)-3,5-bis[(4-dimethylaminophenyl)methylidene]-1-prop-2-enoylpiperidin-4-one) were obtained from the DTI branch at the National Cancer Institute http://dtp.nci.nih.gov/dtpstandard/dwindex/index.jsp. Compounds VLX1545 ((3E,5E)-1-acetyl-3,5-bis[(4-nitrophenyl)methylidene]piperidin-4-one), VLX1547 ((3E,5E)-3,5-bis[(4-fluorophenyl)methylidene]piperidin-4-one), VLX1548 ((3E,5E)-3,5-bis[(4-fluoro-3-hydroxyphenyl)methylidene]piperidin-4-one), VLX1550 ((3E,5E)-3,5-bis[(4-fluorophenyl)methylidene]-1-(prop-2-enoyl)piperidin-4-one) and VLX1554 ((3E,5E)-3,5-bis[(3-hydroxy-4-nitrophenyl)methylidene]-1-(prop-2-enoyl)piperidin-4-one) were synthesized by Oncotargeting AB (Uppsala, Sweden). Ubiquitin vinyl sulfone (U202) was obtained from Boston Biochem (Cambridge, MA).

Cell culture. HCT116 colon carcinoma cells were maintained in McCoy´s 5A modified medium/10% fetal calf serum. A549 cells, HeLa cells and the proteasome reporter cell line MelJuSo Ub-YFP (Menendez-Benito et al., 2005) were cultured in Dulbecco's Modified Eagle's Medium/10 % fetal calf serum. All cells were maintained at 37^{o}C in 5% CO_2 and subcultured by trypsinization.

Cell Viability Assay. Cell viability was monitored either by the FMCA or by the MTT assay. For the FMCA, tumor cells (5,000 cells/well) were seeded in the drug-prepared 384-well plates. Three columns without drugs served as controls and one column with medium

Molecular Pharmacology Fast Forward. Published on April 8, 2014 as DOI: 10.1124/mol.113.091322
This article has not been copyedited and formatted. The final version may differ from this version.

only served as blank. The plates were incubated at 37°C for 72 h and cell viability was then analyzed by measurement of fluorescence from viable cells after 40 min incubation with fluorescein diacetate (FDA). The method is based on measurement of fluorescence generated from hydrolysis of FDA to fluorescein by cells with intact plasma membranes (Lindhagen et al., 2008). Cell survival, expressed as survival index (SI) is defined as fluorescence in test wells divided by fluorescence of control wells, with blank values subtracted, x 100. For the MTT assay, cells were seeded into 96-well flat-bottomed plate overnight and exposed to drugs as described using DMSO as controls. At the end of incubations, 10 µl of a stock solution of 5 mg/ml MTT, was added into each well, and the plates were incubated 4 hours at 37°C. Formazan crystals were dissolved with 100 µl of 10% SDS/10mM HCl solution overnight at 37°C. Absorbance was measured using an ELISA plate reader (Labsystems Multiscan RC) at 590 nm.

Assessment of apoptosis. HCT116 cells were seeded in 96-well microtiter plates at 10,000 cells per well and incubated overnight. Drugs were then added and cells incubated further. At the end of the incubation period, NP40 was added to the tissue culture medium to 0.1% and 25 µl of the content of each well was assayed using the M30-CytoDeath® ELISA (Peviva/VLVbio AB, Sundbyberg, Sweden) (Hägg et al., 2002). This ELISA is based on a specific antibody against a neoepitope of keratin 18 that is generated by the action of caspase-3, -7- and -9 activated in response to apoptosis (Leers et al., 1999).

siRNA knock-down experiments. HeLa cells were maintained in DMEM High Glucose medium with 10% fetal calf serum. For siRNA knockdown cells were transfected with 0.2 µM siRNA (Thermoscientific, Waltham, MA) against USP14, UCHL5 and EGFP as a control sequence. Cells were harvested 48 hours after transfection.

Western blot analysis. Cell extract proteins were resolved by Tris-Acetate PAGE gels (Invitrogen, Carlsbad, CA) and transferred onto a PVDF membrane for western blotting.

Molecular Pharmacology Fast Forward. Published on April 8, 2014 as DOI: 10.1124/mol.113.091322
This article has not been copyedited and formatted. The final version may differ from this version.

Antibodies were obtained from the following sources: anti-USP14 (Bethyl Laboratories, A300-919A); GFP (Cell signaling, #2555), anti-Ubiquitin K48 (Millpore, Apu2); anti-p21(Santa Cruz, sc-756); Hmox-1 (61072), anti-PARP (C2-10), anti-active Caspase 3 (C92-605), anti-β-actin (AC-15) (all from BD Biosciences). Blots were then developed by enhanced chemiluminescence (ECL; Amersham, Arlington Heights, IL).

Analysis of Peroxiredoxin Oxidation. HCT116 cells were plated in 10% FBS McCoy's 5A supplemented with 25 nM selenite overnight (10^6 cells/6-well plate). Following exposure to compounds for the times indicated, cells were washed with degased PBS and incubated for 15 minutes with 180 µl of a peroxiredoxin oxidation inhibition mixture consisting of degased 50 mM Tris pH 7.4, 50 mM NaCl, 1 mM EDTA, 80 mM methyl methanethiosulfonate (Thermo Scientific, 23011), 100 U/ml catalase, and cOmplete EDTA-free protease inhibitor cocktail (Roche, 11873580001). Cells were lysed with the addition of 20 µl 10% NP-40 detergent solution (Thermo Scientific, 28324) on ice for 15 minutes. Cell debris was cleared via centrifugation for 30 minutes at 17,000g, at 4°C, and 20 µg of protein was electrophoresed on a 4 - 20% SDS-PAGE gels under non-reducing conditions and transferred to a nitrocellulose membrane for western blotting. The antibodies used were Prx1 (LF-PA0086), Prx2 (LF-MA0368), and Prx3 (LF-MA0044)(all from Ab Frontier).

Live-cell analysis of UPS-activity. MelJuSo Ub^{G76V}-YFP cells (Menendez-Benito et al., 2005) were plated in black optically clear bottom ViewPlates (PerkinElmer, Waltham, MA, USA) over-night and then exposed to b-AP15 or bortezomib. Treatment with compounds that block the UPS leads to accumulation of YFP in these cells, and the generated fluorescence was continuously detected in an IncuCyte FLR instrument (Essen BioScience Inc., Ann Arbor, MI).

UbVS labeling. HCT116 cells were lysed by freeze-thawing 3X in labeling buffer (50 mM HEPES pH 7.4, 250 mM sucrose, 10 mM MgCl2, 2 mM ATP, 1 mM DTT). After removal of

Molecular Pharmacology Fast Forward. Published on April 8, 2014 as DOI: 10.1124/mol.113.091322
This article has not been copyedited and formatted. The final version may differ from this version.

cell nuclei by centrifugation, total protein (25 μg) was treated with 0, 2.5, 5, 10, 25 and 50 μM b-AP15 for 15 min at 37°C and labeled with Ub-VS (1 μM) for 30 mins at 37°C. Protein concentration was determined using the Bradford assay (BioRad #500-0006). Samples were resolved using SDS-PAGE and subjected to immunoblotting using anti-USP14. Alternatively, total protein extracts (25 μg) were incubated for 15 min at 37°C in labeling buffer in the presence or absence of b-AP15. Extracts were diluted 1 : 20 in labeling buffer containing Ub-VS (1 μM) or b-AP15 and incubation continued at 37°C for 15 min at 37°C. Samples were then subjected to immunoblotting.

Ub-AMC assay. 19S RP (2 nM) were pretreated with DMSO or b-AP15 (6.25, 12.5, 25 or 50 μM) for 2 min in assay buffer (25 mM HEPES, 10 mM $MgCl_2$, 2 mM ATP and 1 mM DTT) before addition of 1 μM Ub-AMC. AMC fluorescence was monitored at 460 nm using an TECAN infinite 200 instrument.

Retention and uptake of b-AP15 in cells. The incorporation of [^{14}C]-bAP15 was monitored using LigandTracer® White according to the instruction of the manufacturer (Ridgeview Instruments AB, Uppsala, Sweden). Briefly, MelJuSo Ub^{G76V}-YFP cells were seeded in a tilted dish to achieve one target area and one cell-free reference area. The dishes were kept tilted in an incubator for 4 - 6 hours, until the cells had adhered. Dishes were then kept horizontally in 10 mL medium to allow the cells to attach firmly to the dish surface for at least 24 hours. The LigandTracer® White instrument were placed in an incubator (37°C in 5% CO_2) before the measurements started for the instrument to reach thermal equilibrium. Culture dishes containing 3 mL cell culture medium and 4 μM [^{14}C]-b-AP15 was placed on the cell dish holder in LigandTracer® White and binding of radioactivity to areas containing cells and reference areas recorded.

TUNEL assay. Apoptotic cells were determined using the APO-BrdU™ TUNEL Assay (Invitogen) according to the manufacturer's Instructions. In briefly, 5×10^5cells/ml cells were

Molecular Pharmacology Fast Forward. Published on April 8, 2014 as DOI: 10.1124/mol.113.091322
This article has not been copyedited and formatted. The final version may differ from this version.

seeded in 6-well plate, then exposed to drugs as described using DMSO as control for 24h. Cells were harvested and fixed in 1% (w/v) paraformaldehyde and 70% (v/v) ethanol, and then incubated in the DNA-labeling solution for 60min at 37°C. This was followed by staining with Alexa Fluor® 488 dye-labeled anti-BrdU antibody and propidium iodide/RNase A solution for 30min at room temperature. Analyze the samples by a BD LSRII flow cytometer (BD Biosciences, San Jose, CA).

Pharmacokinetic studies. Female NMRI mice (20 g) were used. b-AP15 was dissolved in PEG400/CrEL 1 + 1 and diluted 1:10 in saline. The solution was injected in the tail veins of mice (0.4 mg/mL, 2.8 mg/kg). Blood was collected either after 2 min, or after 5 and 15 min (first sample: Vena Saphena, terminal sample: orbital plexus). Ethics approval N476/11 (Stockholm Animal Experimental Ethics committee North). The experiment was performed by Adlego AB (Uppsala, Sweden), record AB-13-34. Plasma samples were thawed at room temperature, mixed with a 2-fold volume of acetonitrile (containing 200 ng/ml of diclofenac as internal standard), shaken and centrifuged for 10 min at 13 000 × g (Heraeus Pico 17 centrifuge), after which supernatants were pipetted to glass vials to wait for the analysis. Standard samples were spiked at 5, 10, 20, 50, 100, 200, 500, 1000 and 2000 nM concentrations in mouse plasma and were otherwise treated as the study samples. Analysis was performed using LC/MS using an Waters Acquity UPLC + Waters Quattro Ultima triple quadrupole MS. These analyses were performed by Admescope (Oulu, Finland).

Hepatocyte metabolism. Pooled cryopreserved human hepatocytes (10-donor mix) and pooled cryopreserved CD-1-mouse hepatocytes (16-donor mix) were obtained from Celsis IVT (product number X008001 and M005052). Samples were analysed by liquid chromatography-mass spectrometry using a Waters Acquity UPLC + Waters Xevo G2 Q-TOF-MS. Waters Acquity C18 (2.1 × 50 mm, 1.7 µm) column with guard filter. Ion chromatograms were extracted from the TOF-MS total ion chromatograms using calculated

Molecular Pharmacology Fast Forward. Published on April 8, 2014 as DOI: 10.1124/mol.113.091322
This article has not been copyedited and formatted. The final version may differ from this version.

monoisotopic accurate masses (calculated using Waters Masslynx software for deprotonated molecule) with 20 mDa window. The metabolites were mined from the data acquired from the last time point, using software-aided data processing (Metabolynx XS including structure-intelligent dealkylation tool & mass defect filter) with manual confirmation. Structures of the observed metabolites are tentatively identified using obtained accurate mass and fragment ion data. This studies were performed by Admescope, Oulu, Finland (investigator: Ari Tolonen, laboratory technicians Birgitta Paldanius and Pirkko Hyvönen).

Enzyme Activity Assays. Recombinant mammalian TrxR1 activity was determined using a DNTB-based colorimetric assay (Arner and Holmgren, 2001). In a 96-well plate, 15 nM TrxR1 was incubated in the presence of 250 μM NADPH (Applichem), 0.1mg/ml BSA, and compounds (1% DMSO) of interest at room temperature for 15 minutes in TE buffer (50 mM Tris-HCl pH 7.5, 2 mM EDTA). Following incubation, 2.5 mM DTNB (in EtOH) was added to each well and reduction of DTNB to TNB^- was followed spectrophotometrically at 412nm using a VersaMax plate reader. GR (Calbiochem#359960) activity was determined in a 96-well plate, with a reaction mixture of 2nM GR incubated in the presence of 250 μM NADPH, 0.1 mg/ml BSA, and compounds of interest at room temperature for 15 minutes in TE buffer. Following incubation, 1mM GSSG was added to each well and NADPH consumption was followed spectrophotometrically at 340 nm.

Cellular TrxR1 Activity. Cellular TrxR1 activity assays were adapted from Eriksson et al (Eriksson et al., 2009). 1.2×10^6 HCT116 cells were plated in a 6-well dish in the presence of 25nM sodium selenite. Following overnight incubation, cells were exposed to b-AP15 (in 0.1% DMSO) for 3 hours. Cells were harvested via trypsinization, suspended in medium containing 10% FBS and centrifuged at 800 rpm for 5 minutes and washed 2X with PBS. Cell pellets were suspended in 200 μl lysis buffer consisting of 50 mM Tris-HCl pH 7.5, 2 mM EDTA, Protease inhibitor cocktail (Roche#11873580001) and 1% Igepal CA-630. Cells were

Molecular Pharmacology Fast Forward. Published on April 8, 2014 as DOI: 10.1124/mol.113.091322
This article has not been copyedited and formatted. The final version may differ from this version.

frozen and thawed 3X using liquid nitrogen followed by 15,000rpm centrifugation at 4°C for 30 minutes. Supernatant was then collected and protein concentration was determined using the Bradford Assay. 5 µg of lysate was incubated in 50 mM Tris-HCl pH 7.5 in the presence of 10 µM Trx1, 275 µM insulin, 1.3 mM NADPH, and 12.5 mM EDTA for 45 minutes at 37°C in a final volume of 50 µl. Samples in a mixture lacking Trx1 were used as a negative control. After incubation, 200 µl 1 mM DTNB in 7.2 M guanidine-HCl was added to each well to stop the enzymatic reaction. Absorbance at 412 nm was determined for each well. Enzymatic activity per mg of protein was determined using the extinction coefficients of DTNB (13,600 $M^{-} cm^{-}$) and NADPH (6200 $M^{-} cm^{-}$).

Statistical analysis. Statistical analysis (Student's T-test, Pearson correlation coefficient or Spearman's rank correlation coefficient as indicated) was performed using Prism software for Apple computers.

Molecular Pharmacology Fast Forward. Published on April 8, 2014 as DOI: 10.1124/mol.113.091322
This article has not been copyedited and formatted. The final version may differ from this version.

Results

Deubiquitinase and proteasome inhibition by b-AP15 in biochemical and cellular assays. The deubiquitinases USP14 and UCHL5 are essential for processing of polyubiquitinated proteins by the proteasome. Knock-down of the expression of both these enzymes in HeLa cells using siRNA resulted in the accumulation of polyubiquitinated proteins (Fig. 1A), consistent with previous findings (Koulich et al., 2008). The small molecule b-AP15 was previously shown to inhibit the activity of USP14 and UCHL5 (D'Arcy et al., 2011). This molecule contains two different types of Michael acceptors, two symmetrically distributed electrophilic α, β-unsaturated carbonyl units (marked by blue symbols in Fig. 1B) and an acrylamide moiety at the central piperidine ring (green symbol in Fig. 1B). The compound VLX1545, where the acrylamide was substituted for an acetamide, elicited a similar degree of cytotoxicity as b-AP15 on HCT116 cells (Fig. 1B, C). Introducing electron donating groups on the side aryls (hydroxyl substituents, VLX1554, Fig. 1B), leading to lower reactivity of the α, β-unsaturated carbonyls (i.e. the Michael acceptors), resulted in a strong decrease in cytotoxicity (Fig. 1B, C). Similar results were found in another series containing fluorides on the side aryls; compound VLX1547 that had no group coupled to the nitrogen atom in the piperidine ring showed a similar anti-proliferative activity as VLX1550 with an acrylamide. The hydroxyl-containing compound VLX1548 showed lower cytotoxic properties. These findings show that the acrylamide is not required for cytotoxicity and identifies the Michael acceptor reactivity of the α, β-unsaturated carbonyl as the pharmacophore regulating biological activity.

We determined the ability of b-AP15 to inhibit proteasome deubiquitinase activity using ubiquitin-AMC as substrate (Fig. 1D). An IC_{50} of 16.8 $\pm$ 2.8 μM was observed. We also used the probe ubiquitin vinyl sulphone (Ub-VS) for activity labeling of USP14. Ub-VS binds

Molecular Pharmacology Fast Forward. Published on April 8, 2014 as DOI: 10.1124/mol.113.091322
This article has not been copyedited and formatted. The final version may differ from this version.

irreversibly to active USP14, resulting in the appearance of a slower migrating form of the protein on Western blots (Fig. 1E). The amount of Ub-VS-labeled USP14 decreased when increasing concentration of b-AP15 were present in the reaction mixture. Quantification of the bands indicated an IC_{50} of ~ 7 μM. In contrast, even at high concentrations (> 50 μM), b-AP15 did not inhibit total deubiquitinase activity in cell extracts or inhibited 20S proteasome activity (not shown; (D'Arcy et al., 2011)).

We next examined inhibition of USP14 in HCT116 cells exposed to b-AP15. Cells were exposed to 1 μM of drug, extracts prepared and labeled with Ub-VS. Inhibition of USP14 and UCHL5 activity was observed under these conditions (Fig. 1F). We consistently found less effective inhibition of UCHL5 in these experiments. Inhibition of cellular proteasome activity was examined using a subline of the human melanoma cell line MelJuSo which expresses a reporter protein (Ub^{G76V}-YFP) degraded by the proteasome. Accumulation of Ub^{G76V}-YFP and of K48-linked ubiquitin-conjugated proteins were observed at concentrations of 0.5 and 1 μM b-AP15 (Fig. 1G). We also noted induction of Hmox-1 at low concentrations of b-AP15 (Fig. 1G), which should relate to induction of oxidative stress (see below).

Accumulation of Ub^{G76V}-YFP was also examined by time-lapse microscopy (Fig. 1H). The majority of cells that became YFP positive showed a rounded, apoptotic morphology after 18 hours of drug exposure (white arrow heads in Fig. 1G). A subpopulation of cells did not become positive; these cells remained viable over the observation period. We conclude that inhibition of proteasome function in cells occurs at concentrations of b-AP15 which are > 10-fold lower than those required for inhibition of deubiquitinase activity in biochemical assays. Further-more, proteasome inhibition correlates to subsequent cell death.

Inhibition of the proteasomal function by b-AP15 is reversible. Deubiquitinase inhibitors having similar structural elements as b-AP15 were reported to be irreversible enzyme inhibitors (Mullally et al., 2001; Zhou et al., 2013). In contrast, we previously

Molecular Pharmacology Fast Forward. Published on April 8, 2014 as DOI: 10.1124/mol.113.091322
This article has not been copyedited and formatted. The final version may differ from this version.

reported reversible inhibition of proteasomal deubiquitinase activity by b-AP15 (D'Arcy et al., 2011). We re-examined the question of reversibility of b-AP15 inhibition of the USP14 deubiquitinase. Active USP14 was labeled with Ub-VS, generating a slower migrating form on SDS-PAGE (Fig. 2A). Addition of 25 μM b-AP15 prior to labeling and during the labeling step inhibited the reaction of Ub-VS with USP14 (slot 4). Addition of 25 μM b-AP15 prior to labeling followed by 20-fold dilution of the extracts (to 1.25 μM) resulted in reappearance of the slower migrating form (slot 5). These data show that binding of b-AP15 to USP14 is indeed reversible.

We next determined whether inhibition of proteasomal function is reversible also in living cells. MelJuSo Ub^{G76V}-YFP cells were exposed to 0.4 μM b-AP15 for 1 hour, followed by medium change and incubation in drug-free medium. As shown in Fig. 2B, high levels of polyubiquitinated proteins were observed after 1 h treatment (time 0) and 1 h after wash-out, but had decreased at 4 h incubation in the absence of drug. The reporter protein Ub^{G76V}-YFP and the proteasome substrate $p21^{Cip1}$ accumulated until 4 h after wash-out, and subsequently decreased. Exposure of MelJuSo Ub^{G76V}-YFP cells to bortezomib for 1 h resulted in transient accumulation of polyubiquitinated proteins (Fig. 2C), consistent with the reversibility of this drug (Adams and Kauffman, 2004).

b-AP15 induces irreversible commitment to cell death. We noticed cleavage of caspase-3 and PARP in cells transiently exposed to b-AP15 and incubated for an additional 23 h (Fig. 2B). This result suggests that despite reversibility of proteasome inhibition, cells became committed to apoptosis after 1 h of exposure to b-AP15. To confirm this finding, we exposed HCT116 cells to b-AP15 for different times and determined caspase-cleaved K18 after 24 h. We indeed found that 1 h of exposure to b-AP15 induced a similar level of caspase-cleaved product as continuous exposure (Fig. 3A). In contrast, bortezomib required longer exposure times to induce apoptosis (Fig. 3A). Using cell viability as an end-point, we found the

Molecular Pharmacology Fast Forward. Published on April 8, 2014 as DOI: 10.1124/mol.113.091322
This article has not been copyedited and formatted. The final version may differ from this version.

difference in IC_{50} values between 1 h and 24 h continuous exposure to b-AP15 to be only ~0.2 μM at both low and high concentrations (Fig. 3B). In contrast, bortezomib reduced viability by < 10% when used at a 400 nM concentration for 1h (Fig. 3C).

Uptake and retention of b-AP15 in cells. The results presented in Fig. 1 show a discrepancy between the potency of b-AP15 to block deubiquitinase activity in biochemical assays versus assays of proteasomal function in cells. We hypothesized that these results may be explained by effective uptake from the medium and enrichment of b-AP15 in the cellular compartment. To examine how b-AP15 distributes from medium to cells we added the compound (1 μM) to culture medium (10% fetal calf serum; 10 mL volume) in the presence or absence of cells and determined the concentration after 1 h incubation at 37°C. A concentration of 1.15 ± 0.005 μM was observed in the culture medium after 1 h incubation in absence of cells, compared to 0.83 ± 0.03 μM in the presence of cells ($p < 0.0001$). This corresponds to a loss of 3.2 nmoles of b-AP15 from the medium (0.32 μM x 10mL). Assuming a cell pellet volume of 50 μL (i.e. 0.5% of culture medium volume), these finding leads to an estimation of an enrichment of b-AP15 in cells of > 50-fold (and a theoretical total intracellular concentration of > 50 μM) over one hour. Determination of free intracellular b-AP15 concentrations showed concentrations in the low nM range, suggesting that the majority of drug molecules are associated with cellular macromolecules (not shown). The results suggest that b-AP15 does not bind strongly to serum proteins in the medium, but rapidly distributes into cells. Consistent with weak binding to serum proteins, the concentration of fetal calf serum in the cell culture medium did not significantly influence the ability of b-AP15 to induce cell death (Fig. 4A).

We next examined the kinetics of cellular uptake of [^{14}C]-b-AP15 using LigandTracer® White (Wang and Albertioni, 2010). Using a b-AP15 concentration of 4 μM, we observed a rapid uptake into cells during 30 minutes of incubation (Fig. 4B, black line). Following wash-

Molecular Pharmacology Fast Forward. Published on April 8, 2014 as DOI: 10.1124/mol.113.091322
This article has not been copyedited and formatted. The final version may differ from this version.

out of substance, ~ 40% of the [^{14}C]-b-AP15 signal disappeared during 2 h. After 10 h, ~ 50% of the radioactivity remained associated with cells (Supplementary Fig. 1). Pre-treating cells with 10 μM N-ethylmaleimide for 30 min prior to addition of [^{14}C]-b-AP15 resulted in an ~ 80% decrease in binding (Fig. 4B, red line).

The finding that a significant amount of drug remains associated with cells several hours after washing out leads to the prediction that at high drug concentrations a sufficient number of drug molecules will be available for inhibiting the proteasome also after wash-out. To test this prediction, we examined the reversibility of proteasome function in cells using increasing concentrations of b-AP15. We indeed found that after exposing MelJuSo cells to 0.8 or 1 μM b-AP15 for 1 h, polyubiquitin remained 8 hours after changing to drug-free medium (Fig. 4C).

Pharmacokinetics and metabolism. We injected b-AP15 (dissolved in PEG400/Chremophor EL/saline 5/5/90) into NMRI mice and determined drug concentrations in plasma by mass spectrometry. An half-life of < 5 min was observed in plasma (Fig. 5A). This rapid clearance of b-AP15 from plasma is consistent with the rapid uptake into cells described above.

Metabolite profiling in mouse and human hepatocytes was performed using 3 h incubation time. A total of 23 metabolites of b-AP15 were observed, 17 in human and 19 in mouse hepatocytes. The observed metabolic reactions included several hydrogenation reactions, together with further hydroxylation reactions and/or glucuronide conjugations. In addition, S-glutathione (GSH) and S-cysteine conjugates after various hydrogenation reactions were observed. As expected, biotransformation sites for hydrogenation reactions were located to the electrophilic α, β-unsaturated carbonyl units. The different metabolites are shown in Fig. 5B and the relative abundance of each metabolite is shown in Table 1.

Elevated induction of oxidative stress by b-AP15 is partially dissociated from

Molecular Pharmacology Fast Forward. Published on April 8, 2014 as DOI: 10.1124/mol.113.091322
This article has not been copyedited and formatted. The final version may differ from this version.

proteasome inhibition. A hypothetical intracellular concentration of b-AP15 of ~ 50 μM is consistent with binding to a considerable fraction of intracellular thiols (estimated to be in the order of 1 - 5 mM (Di Monte et al., 1984)). Although proteasomes are abundant in cells (~ 1% of cellular protein (Tanaka and Ichihara, 1989)), it is unlikely that b-AP15 binds exclusively to proteasomal deubiquitinases in cells. Defining additional cellular targets is important for understanding the activity profile of the drug. Bortezomib is known to induce oxidative stress (Ling et al., 2003) and increases the expression of the oxidative stress-associated marker Hmox-1 (Brnjic et al., 2013; Hamamura et al., 2007). As previously reported (Brnjic et al., 2013), b-AP15 induced a stronger increase in Hmox-1 compared to bortezomib (Fig. 6A). During the course of this study we noticed that Hmox-1 was induced by 0.2 μM b-AP15 (Fig. 1G), a drug concentration that elicits limited proteasome inhibition and cytotoxicity. This observation raised the possibility that the oxidative stress response may be at least partially dissociated from proteasome inhibition.

To further examine whether proteasome inhibition and oxidative stress can be dissociated, we examined the response to a number of b-AP15 analogues (Fig. 6, Supplementary Fig. 2). Similar to b-AP15, compounds b-AP107, VLX1545 and VLX1548 also induced Hmox-1 expression at concentrations that did not induce caspase-3 cleavage (Fig. 6A). The analogues b-AP113, VLX1547 and VLX1550 induced little or no accumulation polyubiquitin and did not induce strong caspase-3 cleavage or TUNEL positivity at the concentrations used in Fig. 6A and B. In contrast, these compounds all induced Hmox-1 expression (Fig. 6A). The results show that b-AP15-related compounds induce oxidative stress by a mechanism that is partially distinct from proteasome inhibition, and that oxidative stress is not sufficient to induce apoptosis.

Compound b-AP113 induces Hmox-1 but not apoptosis at concentrations of 10 and 20 μM over 18-24 hours (Fig. 6). To examine whether oxidative stress induction by this compound

Molecular Pharmacology Fast Forward. Published on April 8, 2014 as DOI: 10.1124/mol.113.091322
This article has not been copyedited and formatted. The final version may differ from this version.

kills cells by other cell death modes (e.g. necrosis) over longer time periods, we used an IncuCyte instrument (Essen Biosciences) to follow cell growth and Ub^{G76V}-YFP accumulation. At a concentration of 10 μM, b-AP113 did not affect MelJuSo cell viability over 72 hours (Supplementary Fig. 3).

b-AP15 is an irreversible inhibitor of thioredoxin reductase. The thioredoxin and glutathione systems are essential for cellular redox-homeostasis. Cyclopentenone prostaglandins have previously been found to inhibit the activity of thioredoxin reductase (TrxR) (Moos et al., 2003; Shibata et al., 2003), suggesting to us that b-AP15 may possibly also target TrxR. TrxR enzymatic activity is dependent on the motif Gly-Cys-Sec-Gly, where Sec is selenocysteine, while glutathione reductase (GR) activity is dependent on the two cysteine residues Cys58 and Cys63 (Berkholz et al., 2008). The Sec residue of TrxR is particularly reactive to electrophiles (Rundlof and Arner, 2004) and inhibition of TrxR typically induces Hmox-1 expression (Mostert et al., 2003). As shown in Fig. 7A, TrxR activity is inhibited by b-AP15 in HCT116 cells exposed to b-AP15. Furthermore, TrxR activity was inhibited by b-AP15 in an *in vitro* assay at a concentration of ~1 μM (Fig. 7B). In contrast, GR activity was not significantly inhibited. Compounds b-AP107, b-AP113**,** VLX1545, VLX1547 and VLX1550 also inhibited TrxR1 activity with somewhat different potencies (Fig. 7B), whereas compounds VLX1548 and VLX1554 did not inhibit TrxR activity at the concentrations tested. Bortezomib did not inhibit TrxR or GR activity (Fig. 7B). We conclude that b-AP15 and some of its analogues inhibit TrxR and induce Hmox-1 expression. Furthermore, the relatively low ability of VLX1554 to induce Hmox-1 (Fig. 6) correlated with weak inhibition of TrxR. We also conclude that bortezomib induces Hmox-1 expression without apparent inhibition of TrxR.

We next examined whether b-AP15 is an irreversible inhibitor of TrxR. Enzyme activity was determined before and after desalting by gel filtration. As shown in Fig. 7C, inhibition of

Molecular Pharmacology Fast Forward. Published on April 8, 2014 as DOI: 10.1124/mol.113.091322
This article has not been copyedited and formatted. The final version may differ from this version.

TrxR by b-AP15 remained after gel filtration, showing irreversible inhibition.

Thioredoxin reductase inhibition does not appear to be essential for the cytotoxicity or proteasome inhibition by b-AP15. Two features that distinguish the response to b-AP15 and bortezomib is the more rapid kinetics of apoptosis induction by b-AP15 and the ability of this compound to induce apoptosis in cells overexpressing Bcl-2 (Brnjic et al., 2013; D'Arcy et al., 2011). In order to examine whether these differences may be accounted for by the inhibition of TrxR by b-AP15, we combined bortezomib with the TrxR inhibitor auranofin. At 14 h of exposure, b-AP15 induced an ~ 5-fold increase in caspase-cleaved K18, compared to 2 - 3 fold by bortezomib (Fig. 7D). The combination of bortezomib and auranofin did not generate a similar apoptotic response as b-AP15 alone. Similarly, whereas b-AP15 induced an apoptotic response in HCT116 cells overexpressing Bcl-2, bortezomib did not (Fig. 7E). Auranofin increased the effect of bortezomib at a 14 h time-point, but the effect of the combination was not as strong as that of b-AP15 alone (Fig. 7E). These results demonstrate that although TrxR inhibition by b-AP15 is likely to contribute to oxidative stress and apoptosis, this activity can not by itself explain the strong apoptotic activity of this compound.

A TrxR-related protein has been found to be associated with the proteasome (Wiseman et al., 2009). We therefore examined whether TrxR inhibition influences proteasome function in tumor cells. As shown in Fig. 7F, auranofin did not induce a similar degree of polyubiquitin accumulation in HCT116, A549 or MelJuSo cells as b-AP15. Furthermore, auranofin did not induce Ub^{G76V}-YFP accumulation in MelJuSo cells. Auranofin consistently induced higher levels of Hmox-1 compared to b-AP15 in these different cell lines. A549 cells show constitutive Nrf-2 activity, resulting in baseline Hmox-1 expression. b-AP15 and auranofin induced dimerization of periredoxin-3, showing oxidative stress (Poynton and Hampton, 2014), whereas bortezomib did not (Supplementaty Figure 4). We conclude that TrxR inhibition or Hmox-1 induction are events that are not necessarily linked to impaired

Molecular Pharmacology Fast Forward. Published on April 8, 2014 as DOI: 10.1124/mol.113.091322
This article has not been copyedited and formatted. The final version may differ from this version.

proteasome function.

Molecular Pharmacology Fast Forward. Published on April 8, 2014 as DOI: 10.1124/mol.113.091322
This article has not been copyedited and formatted. The final version may differ from this version.

Discussion

Previous work demonstrated that the small molecule b-AP15 inhibits USP14/UCHL5 deubiquitinase activity and shows promising anti-tumor activity in syngeneic and xenograft tumor models (D'Arcy et al., 2011). b-AP15 induces accumulation of high-molecular weight polyubiquitin in the submicromolar range. In contrast, inhibition of deubiquitinase activity *in vitro* is observed at concentrations of ~ 10 μM. We here provide an explanation for this apparent discrepancy by showing that b-AP15 is strongly enriched in cells. Enrichment appears to be driven by thiol-dependent mechanisms, as evidenced by inhibition of uptake by short pre-treatment of cells with low concentrations of N-ethylmaleimide. Concentrations of free b-AP15 in cells were low (1 - 5 nM), consistent with intracellular covalent binding of the compound to thiols. In contrast to the rapid sequestration to intracellular thiols, free b-AP15 was recovered from cell culture medium containing fetal calf serum, showing that the compound did not irreversibly bind serum proteins. Furthermore, increasing the fetal calf serum concentration in the culture medium did not significantly decrease the cytotoxic activity of b-AP15. Our findings suggest that b-AP15 is rapidly distributed from serum/plasma to cellular compartments both in cell cultures and in exposed mice.

b-AP15 belongs to a class of compounds that contain α, β-unsaturated carbonyl groups and that inhibit cellular deubiquitinases. The compound also contains a potentially reactive acrylamide residue, but this group was not necessary for cytotoxic activity in colon cancer cells and was not found to be modified in hepatocytes. We have synthesized a number of compounds where various groups were coupled to the α, β-unsaturated carbonyls. These compounds show cytotoxic activities in the 5 - 10 μM range (unpublished data) and we assume that the side groups are released. The side-aryls of b-AP15 are substituted with electron withdrawing $–NO_2$ groups which increase the Michael acceptor capability of the α, β-

Molecular Pharmacology Fast Forward. Published on April 8, 2014 as DOI: 10.1124/mol.113.091322
This article has not been copyedited and formatted. The final version may differ from this version.

unsaturated carbonyls. As expected, introduction of electron-donating groups on the side-aryls (b-AP113, VLX1554 and VLX1558), significantly impaired the proteasome inhibiting and cytotoxic activity of these compounds, presumably by decreasing the reactivity of the α, β-unsaturated carbonyls. Other compounds containing similar structural elements as b-AP15 were reported to show different specificities with regard to deubiquitinase inhibition. Prostaglandin 12δ-PGJ2 was reported to inhibit UCHL1 and UCHL3 (Li et al., 2004) and WP1130 inhibits USP9x, USP5, USP14 and UCHL5 (Kapuria et al., 2010). Similar to b-AP15, the compound AC17 was found to specifically inhibit proteasomal deubiquitinases (Zhou et al., 2013). The mechanisms underlying these different specificities are unclear, but presumably reflect the accessibility of cysteines in the active sites of different deubiquitinases to these small molecules. It remains to be explained how both USP and UCH classes of deubiquitinases, which show limited homology (Komander et al., 2009), can be inhibited by these compounds. We generally find more effective inhibition of USP14 compared to UCHL5 both in cell extracts and using 19S proteasomes (data not shown), raising the possibility that USP14 is the most high affinity target for b-AP15.

Target residence time is known to be affected by the context of the reactive electrophile (Serafimova et al., 2012). Compounds having similar electrophiles as b-AP15 (i.e. α, β-unsaturated carbonyl chains) were reported to be irreversible deubiquitinase inhibitors (Mullally and Fitzpatrick, 2002; Zhou et al., 2013). Cyclopentenone prostaglandins containing Michael acceptors bind soluble cysteine thiols such as cysteine and glutathione in a reversible manner, whereas the solid state Michael reaction is less reversible, possibly due to decreased molecular motion (Suzuki et al., 1997). Binding of b-AP15 to USP14 is reversible (Fig. 2), consistent with our previous results (D'Arcy et al., 2011). The α, β-unsaturated carbonyl conjugated system in b-AP15 is apparently prone to retro-Michael reactions under some conditions. At low concentrations (0.4 and 0.6 μM), transient exposure to b-AP15 lead to

Molecular Pharmacology Fast Forward. Published on April 8, 2014 as DOI: 10.1124/mol.113.091322
This article has not been copyedited and formatted. The final version may differ from this version.

disappearance of polyubiquitin after 8 hours of incubation in drug-free medium (Fig. 2 and 4). Interestingly, cells nevertheless become committed to apoptosis/cell death (Fig. 2 and 3). We do not presently understand the mechanism of this rapid and seemingly faithful commitment. At higher concentrations (0.8 and 1 μM), polyubiquitin conjugates did not disappear in transiently exposed cells. We interpret this result to suggest that a sufficient number of drug molecules are present in cells to be able to continuously inhibit proteasomal deubiquitinases. The slow release of the compound from cells (Fig. 4B) is consistent with this assumption. In contrast to the rapid commitment to cell death by b-AP15, transient exposure to bortezomib did not result in apoptosis/cell death (Fig. 3C). Promising *in vivo* activities of b-AP15 has been observed in a number of tumor models (D'Arcy et al., 2011; Tian et al., 2013), and this activity may partially be due to the ability of the compound to induce cell death after relatively short periods of exposure.

Michael acceptors are traditionally avoided by drug developers due to their reactivity. However, many biologically relevant pathways are targeted by thiol-reactive compounds and covalent coupling to thiols is a potentially important mechanism of bioactivity (Amslinger, 2010). An irreversible inhibitor of the AAA family ATPase VCP (p97/Cdc48p) was recently described (Magnaghi et al., 2013). This compound (NMS-873) covalently modifies an active site cysteine of this enzyme. Similar to b-AP15, NMS-873 induced accumulation of polyubiquitin and cancer cell death. The homo-triterpenoid bardoxolone methyl (RTA402) contains and α, β-unsaturated carbonyl unit (Liby et al., 2007) and is in clinical development for the treatment of diabetes-associated chronic kidney disease (Pergola et al., 2011). Bardoxolone methyl has also been given orphan drug status by the FDA for the treatment of pancreatic cancer (http://www.news-medical.net/news/2008/10/16/42030.aspx).

We here report that in addition to inhibition of proteasome function, b-AP15 inhibits TrxR. The active site of this enzyme contains a selenocysteine residue which is reactive to

Molecular Pharmacology Fast Forward. Published on April 8, 2014 as DOI: 10.1124/mol.113.091322
This article has not been copyedited and formatted. The final version may differ from this version.

electrophiles (Rundlof and Arner, 2004) and TrxR inhibition by b-AP15 is therefore not surprising. In contrast to inhibition of USP14, inhibition of TrxR was found to be irreversible, possibly reflecting the strong reactivity of the drug to the enzyme. In contrast, GR enzyme activity was not inhibited. GR activity is dependent on two cysteine residues (Cys58 and Cys63) (Berkholz et al., 2008). The TrxR over GR selectivity of b-AP15 shows specificity for some cysteines, and is consistent with previous reports that electrophilic compounds selectively react with cellular cysteines (Dennehy et al., 2006; Liebler, 2008) and the fact that TrxR, with its selenocysteine residue, is particularly prone to inhibition by electrophiles, including prostaglandin derivatives (Moos et al., 2003). The bioactive cyclopentenone 15δ-PGJ2, known to induce cellular oxidative stress, has been shown to inhibit TrxR activity (Shibata et al., 2003). Contrary to expectation, 15δ-PGJ2 was reported to bind Cys-35 or Cys-69, and not Sec, in TrxR (Shibata et al., 2003). We do not presently know which cysteine residue in TrxR that is targeted by b-AP15. We previously reported that oxidative stress is an important mediator of apoptosis induction by b-AP15 (Brnjic et al., 2013), and it is likely that TrxR inhibition contributes to apoptotic signaling. Since bortezomib induces oxidative stress in the absence of TrxR inhibition, we hypothesize that the strong oxidative stress observed in cells exposed to b-AP15 is due to both proteasome and TrxR inhibition. Our experiments combining bortezomib and auranofin suggested that TrxR inhibition contributes to the apoptotic activity of b-AP15, but is of limited importance for the superior cytotoxicity of b-AP15 over bortezomib. We also found that TrxR inhibition is unlikely to contribute to proteasome inhibition by b-AP15. This was important to establish in the light of reports showing that TRP32 (thioredoxin-related protein of 32 kDa; TXNL1) is a subunit of the 26 S proteasome and that auranofin treatment changes the expression of proteasomal proteins (Guidi et al., 2012).

The present study has clarified a number of questions with regard to the mechanism of

Molecular Pharmacology Fast Forward. Published on April 8, 2014 as DOI: 10.1124/mol.113.091322
This article has not been copyedited and formatted. The final version may differ from this version.

action and pharmacology of the deubiquitinase inhibitor b-AP15. The findings of rapid uptake and enrichment in cells and the commitment to apoptosis/cell death within one hour lead to some optimism with regard to clinical activity of b-AP15 (or optimized leads of this compound).

Molecular Pharmacology Fast Forward. Published on April 8, 2014 as DOI: 10.1124/mol.113.091322
This article has not been copyedited and formatted. The final version may differ from this version.

Acknowledgements

We acknowledge Admescope, Oulu, Finland for the performance of LC/MS (pharmacokinetic studies) and metabolism studies. We acknowledge OncoTargeting, Uppsala, Sweden, for synthesis of compounds. We are also grateful to Hans Rosén, Vivolux AB, for support and input at various levels as well as organizational help. We acknowledge Adlego AB, Uppsala, for performance of pharmacokinetic studies. Arne Holmgren kindly provided Trx1. We acknowledge the Developmental Therapeutics Branch at the National Cancer Institute, Bethesda, for supplying compounds. We are grateful to Maria Rydåker, Lena Lenhammar and Christina Leek for excellent technical support.

Molecular Pharmacology Fast Forward. Published on April 8, 2014 as DOI: 10.1124/mol.113.091322
This article has not been copyedited and formatted. The final version may differ from this version.

Author contributions

Participated in research design: Wang, Stafford, Gullbo, Arnér, Larsson, Brnjic, Fryknäs, D'Arcy, Linder.

Conducted experiments: Wang, Stafford, Mazurkiewicz, Fryknäs, Brjnic, Zhang, D'Arcy.

Performed data analysis: Wang, Stafford, Mazurkiewicz, Fryknäs, Brjnic, Zhang, Gullbo, Larsson, Arnér, D'Arcy, Linder.

Wrote or contributed to the writing of the manuscript: Wang, Stafford, Mazurkiewicz, Fryknäs, Brjnic, Zhang, Gullbo, Larsson, Arnér, D'Arcy, Linder.

Molecular Pharmacology Fast Forward. Published on April 8, 2014 as DOI: 10.1124/mol.113.091322
This article has not been copyedited and formatted. The final version may differ from this version.

References

Adams J (2001) Proteasome inhibition in cancer: development of PS-341. *Seminars in oncology* **28**: 613-619.

Adams J, and Kauffman M (2004) Development of the proteasome inhibitor Velcade (Bortezomib). *Cancer Invest* **22**: 304-311.

Aleo E, Henderson CJ, Fontanini A, Solazzo B, and Brancolini C (2006) Identification of new compounds that trigger apoptosome-independent caspase activation and apoptosis. *Cancer research* **66**: 9235-9244.

Amslinger S (2010) The tunable functionality of alpha,beta-unsaturated carbonyl compounds enables their differential application in biological systems. *ChemMedChem* **5**: 351-356.

Arner ES, and Holmgren A (2001) Measurement of thioredoxin and thioredoxin reductase. *Curr Protoc Toxicol* Chapter **7**: Unit 7 4.

Berkholz DS, Faber HR, Savvides SN, and Karplus PA (2008) Catalytic cycle of human glutathione reductase near 1 A resolution. *J Mol Biol* **382**: 371-384.

Brnjic S, Mazurkiewicz M, Fryknas M, Sun C, Zhang X, Larsson R, D'Arcy P, and Linder ST (2013) Induction of tumor cell apoptosis by a proteasome deubiquitinase inhibitor is associated with oxidative stress. *Antioxid Redox Signal*.

Caravita T, de Fabritiis P, Palumbo A, Amadori S, and Boccadoro M (2006) Bortezomib: efficacy comparisons in solid tumors and hematologic malignancies. *Nat Clin Pract Oncol* **3**: 374-387.

Chauhan D, Hideshima T, and Anderson KC (2005) Proteasome inhibition in multiple myeloma: therapeutic implication. *Annu Rev Pharmacol Toxicol* **45**: 465-476.

D'Arcy P, Brnjic S, Olofsson MH, Fryknas M, Lindsten K, De Cesare M, Perego P, Sadeghi B, Hassan M, Larsson R, and Linder S (2011) Inhibition of proteasome deubiquitinating activity as a new cancer therapy. *Nature medicine* **17**: 1636-1640.

Dennehy MK, Richards KA, Wernke GR, Shyr Y, and Liebler DC (2006) Cytosolic and nuclear protein targets of thiol-reactive electrophiles. *Chem Res Toxicol* **19**: 20-29.

Di Monte D, Ross D, Bellomo G, Eklow L, and Orrenius S (1984) Alterations in intracellular thiol homeostasis during the metabolism of menadione by isolated rat hepatocytes. *Arch Biochem Biophys* **235**: 334-342.

Eriksson SE, Prast-Nielsen S, Flaberg E, Szekely L, and Arnér ESJ (2009) High levels of thioredoxin reductase 1 modulate drug-specific cytotoxic efficacy. *Free Radical Biology and Medicine* **47**: 1661-1671.

Groll M, Heinemeyer W, Jager S, Ullrich T, Bochtler M, Wolf DH, and Huber R (1999) The catalytic sites of 20S proteasomes and their role in subunit maturation: a mutational and crystallographic study. *Proc Natl Acad Sci U S A* **96**: 10976-10983.

Guidi F, Landini I, Puglia M, Magherini F, Gabbiani C, Cinellu MA, Nobili S, Fiaschi T, Bini L, Mini E, Messori L, and Modesti A (2012) Proteomic analysis of ovarian cancer cell responses to cytotoxic gold compounds. *Metallomics* **4**: 307-314.

Hägg M, Biven K, Ueno T, Rydlander L, Bjorklund P, Wiman KG, Shoshan M, and Linder S (2002) A novel high-through-put assay for screening of pro-apoptotic drugs. *Invest New Drugs* **20**: 253-259.

Hamamura RS, Ohyashiki JH, Kurashina R, Kobayashi C, Zhang Y, Takaku T, and Ohyashiki K (2007) Induction of heme oxygenase-1 by cobalt protoporphyrin

enhances the antitumour effect of bortezomib in adult T-cell leukaemia cells. *Br J Cancer* **97**: 1099-1105.

Hershko A, and Ciechanover A (1998) The ubiquitin system. *Annual review of biochemistry* **67**: 425-479.

Kapuria V, Peterson LF, Fang D, Bornmann WG, Talpaz M, and Donato NJ (2010) Deubiquitinase inhibition by small-molecule WP1130 triggers aggresome formation and tumor cell apoptosis. *Cancer research* **70**: 9265-9276.

Komander D, Clague MJ, and Urbe S (2009) Breaking the chains: structure and function of the deubiquitinases. *Nature reviews Molecular cell biology* **10**: 550-563.

Koulich E, Li X, and DeMartino GN (2008) Relative structural and functional roles of multiple deubiquitylating proteins associated with mammalian 26S proteasome. *Mol Biol Cell* **19**: 1072-1082.

Lee MJ, Lee BH, Hanna J, King RW, and Finley D (2011) Trimming of ubiquitin chains by proteasome-associated deubiquitinating enzymes. *Mol Cell Proteomics* **10**: R110 003871.

Leers MP, W K, Björklund V, Bergman T, Tribbick G, Persson B, Björklund P, Ramaekers FC, Björklund B, Nap M, H J, and Schutte B (1999) Immunocytochemical detection and mapping of a cytokeratin 18 neo-epitope exposed during early apoptosis. *J Pathol* **187**: 567-572.

Li Z, Melandri F, Berdo I, Jansen M, Hunter L, Wright S, Valbrun D, and Figueiredo-Pereira ME (2004) Delta12-Prostaglandin J2 inhibits the ubiquitin hydrolase UCH-L1 and elicits ubiquitin-protein aggregation without proteasome inhibition. *Biochem Biophys Res Commun* **319**: 1171-1180.

Liby KT, Yore MM, and Sporn MB (2007) Triterpenoids and rexinoids as multifunctional agents for the prevention and treatment of cancer. *Nature reviews Cancer* **7**: 357-369.

Liebler DC (2008) Protein damage by reactive electrophiles: targets and consequences. *Chem Res Toxicol* **21**: 117-128.

Lindhagen E, Nygren P, and Larsson R (2008) The fluorometric microculture cytotoxicity assay. *Nat Protoc* **3**: 1364-1369.

Ling YH, Liebes L, Zou Y, and Perez-Soler R (2003) Reactive oxygen species generation and mitochondrial dysfunction in the apoptotic response to Bortezomib, a novel proteasome inhibitor, in human H460 non-small cell lung cancer cells. *The Journal of biological chemistry* **278**: 33714-33723.

Magnaghi P, D'Alessio R, Valsasina B, Avanzi N, Rizzi S, Asa D, Gasparri F, Cozzi L, Cucchi U, Orrenius C, Polucci P, Ballinari D, Perrera C, Leone A, Cervi G, Casale E, Xiao Y, Wong C, Anderson DJ, Galvani A, Donati D, O'Brien T, Jackson PK, and Isacchi A (2013) Covalent and allosteric inhibitors of the ATPase VCP/p97 induce cancer cell death. *Nat Chem Biol* **9**: 548-556.

Menendez-Benito V, Verhoef LG, Masucci MG, and Dantuma NP (2005) Endoplasmic reticulum stress compromises the ubiquitin-proteasome system. *Hum Mol Genet* **14**: 2787-2799.

Moos PJ, Edes K, Cassidy P, Massuda E, and Fitzpatrick FA (2003) Electrophilic prostaglandins and lipid aldehydes repress redox-sensitive transcription factors p53 and hypoxia-inducible factor by impairing the selenoprotein thioredoxin reductase. *The Journal of biological chemistry* **278**: 745-750.

Mostert V, Hill KE, Ferris CD, and Burk RF (2003) Selective induction of liver parenchymal cell heme oxygenase-1 in selenium-deficient rats. *Biological chemistry* **384**: 681-687.

Mullally JE, and Fitzpatrick FA (2002) Pharmacophore model for novel inhibitors of ubiquitin isopeptidases that induce p53-independent cell death. *Mol Pharmacol* **62**: 351-358.

Mullally JE, Moos PJ, Edes K, and Fitzpatrick FA (2001) Cyclopentenone prostaglandins of the J series inhibit the ubiquitin isopeptidase activity of the proteasome pathway. *The Journal of biological chemistry* **276**: 30366-30373.

Pergola PE, Raskin P, Toto RD, Meyer CJ, Huff JW, Grossman EB, Krauth M, Ruiz S, Audhya P, Christ-Schmidt H, Wittes J, and Warnock DG (2011) Bardoxolone methyl and kidney function in CKD with type 2 diabetes. *N Engl J Med* **365**: 327-336.

Poynton RA, and Hampton MB (2014) Peroxiredoxins as biomarkers of oxidative stress. *Biochimica et biophysica acta* **1840**: 906-912.

Rundlof AK, and Arner ES (2004) Regulation of the mammalian selenoprotein thioredoxin reductase 1 in relation to cellular phenotype, growth, and signaling events. *Antioxid Redox Signal* **6**: 41-52.

Serafimova IM, Pufall MA, Krishnan S, Duda K, Cohen MS, Maglathlin RL, McFarland JM, Miller RM, Frodin M, and Taunton J (2012) Reversible targeting of noncatalytic cysteines with chemically tuned electrophiles. *Nat Chem Biol* **8**: 471-476.

Shibata T, Yamada T, Ishii T, Kumazawa S, Nakamura H, Masutani H, Yodoi J, and Uchida K (2003) Thioredoxin as a molecular target of cyclopentenone prostaglandins. *The Journal of biological chemistry* **278**: 26046-26054.

Suzuki M, Mori M, Niwa T, Hitrata R, Furuta K, Ishikawa T, and Noyori R (1997) Chemical Implications for Antitumor and Antiviral Prostaglandins: Reaction of D7-Prostaglandin A1 and Prostaglandin A1 Methyl Esters with Thiols. *J Am Chem Soc* **119**: 2376-2385.

Tanaka K, and Ichihara A (1989) Half-life of proteasomes (multiprotease complexes) in rat liver. *Biochem Biophys Res Commun* **159**: 1309-1315.

Tian Z, D'Arcy P, Wang X, Ray A, Tai YT, Hu Y, Carrasco RD, Richardson P, Linder S, Chauhan D, and Anderson KC (2013) A novel small molecule inhibitor of deubiquitylating enzyme USP14 and UCHL5 induces apoptosis in multiple myeloma and overcomes bortezomib resistance. *Blood* **125**: 706-716.

Verma R, Aravind L, Oania R, McDonald WH, Yates JR, 3rd, Koonin EV, and Deshaies RJ (2002) Role of Rpn11 metalloprotease in deubiquitination and degradation by the 26S proteasome. *Science* **298**: 611-615.

Voorhees PM, and Orlowski RZ (2006) The proteasome and proteasome inhibitors in cancer therapy. *Annu Rev Pharmacol Toxicol* **46**: 189-213.

Wang X, and Albertioni F (2010) Effect of clofarabine on apoptosis and DNA synthesis in human epithelial colon cancer cells. *Nucleosides Nucleotides Nucleic Acids* **29**: 414-418.

Wiseman RL, Chin KT, Haynes CM, Stanhill A, Xu CF, Roguev A, Krogan NJ, Neubert TA, and Ron D (2009) Thioredoxin-related Protein 32 is an arsenite-regulated Thiol Reductase of the proteasome 19 S particle. *J Biol Chem* **284**: 15233-15245.

Yao T, and Cohen RS (2002) A cryptic protease couples deubiquitinylation and degradation by the proteasome. *Nature* **419**: 403-407.

Zhou B, Zuo Y, Li B, Wang H, Liu H, Wang X, Qiu X, Hu Y, Wen S, Du J, and Bu X (2013) Deubiquitinase inhibition of 19S regulatory particles by 4-arylidene curcumin analog AC17 causes NF-kappaB inhibition and p53 reactivation in human lung cancer cells. *Molecular cancer therapeutics* **12**: 1381-1392.

Molecular Pharmacology Fast Forward. Published on April 8, 2014 as DOI: 10.1124/mol.113.091322
This article has not been copyedited and formatted. The final version may differ from this version.

Footnote: The work was supported by Cancerfonden, Radiumhemmets Forskningsfonder, Vetenskapsrådet, Barncancerfonden and Strategiska Forskningsstiftelsen (SSF).

Molecular Pharmacology Fast Forward. Published on April 8, 2014 as DOI: 10.1124/mol.113.091322
This article has not been copyedited and formatted. The final version may differ from this version.

Legends for figures

Fig. 1. b-AP15 inhibits deubiquitinase activity and proteasome function. (A) Knock-down of USP14 and UCHL5 leads to accumulation of polyubiquitinated proteins in HCT116 cells. Cells were transfected with siRNA over-night, incubated for a further 48 h and processed for western blotting. HCT116 is a colon carcinoma cell line previously found to the sensitive to b-AP15 (D'Arcy et al., 2011). Note that single siRNAs did not induce polyubiquitin accumulation, nor did scrambled siRNAs (not shown); (B) Molecular structure of b-AP15 (NSC687852) and various analogues. The α, β-unsaturated carbonyls are marked with blue filled circles and the Michael acceptor at the acrylamide with a green circle. The asterix marks the position of the [^{14}C] in the labeled b-AP15 used in Fig. 4. (C) Dose-response determinations to b-AP15 and various analogues. HCT116 cell viability was determined after 72 h of exposure using FMCA. The results are expressed as percentage of the untreated control and presented as mean values +/- standard deviation. (D) 19S RP (2nM) were pretreated with DMSO or b-AP15 (6.25, 12.5, 25 or 50μM) for 2 min in assay buffer before addition of 1μM Ub-AMC. Fluorescence was then recorded continuously. (E) Inhibition of Ub-VS labeling of USP14 by b-AP15. HCT116 cell extracts (25μg protein) were incubated with the indicated concentrations of b-AP15 and subsequently incubated with Ub-VS. Samples were subjected to western blotting using an USP14 antibody. (F) Inhibition of USP14 and UCHL5 in HCT116 cells. HCT116 cells were exposed to 1 μM b-AP15 for 6 h and lysed. Extracts (25 μg) were labeled with Ub-VS (25 μM) for 5 min at 37°C. Samples were subjected to western blotting using USP14 and UCHL5 antibodies. (G) Accumulation of polyubiquitin and Ub^{G76V}-YFP in MelJuSo cells exposed to b-AP15. The Ub^{G76V}-YFP fusion protein is degraded by the proteasome under normal conditions. Note that Hmox-1 is induced at concentrations which do not block the proteasome. (H) Analysis of accumulation of Ub^{G76V}-YFP

Molecular Pharmacology Fast Forward. Published on April 8, 2014 as DOI: 10.1124/mol.113.091322
This article has not been copyedited and formatted. The final version may differ from this version.

in MelJuSo cells following exposure to 0.5 μM b-AP15. Note that YFP-positive cells die during the period of observation (white arrow heads), whereas cells remaining YFP negative are unaffected.

Molecular Pharmacology Fast Forward. Published on April 8, 2014 as DOI: 10.1124/mol.113.091322
This article has not been copyedited and formatted. The final version may differ from this version.

Fig. 2. b-AP15 is a reversible inhibitor of USP14 *in vitro* and of proteasome function in cells. (A) Reversibility of b-AP15 inhibition of USP14. Total HCT116 cell extracts were prepared and first incubated for 15 min at 37^{o}C in the presence or absence of 25 μM b-AP15 (pre-labeling step). Ub-VS (1 μM) was added and incubation continued in the presence or absence of b-AP15 for 15 min (slot 2 -3). Extracts were diluted 1 : 20 in labeling buffer and 1 μM Ub-VS was added (slot 5) and incubation continued for 15 min. After 30 min incubation was terminated and samples were prepared for immunoblotting using an USP14 antibody. Note that b-AP15 inhibits labeling of USP14 when present at 25 μM, but that this effect is reversed after dilution of the extracts to 1.25 μM. (B) Reversibility of proteasome inhibition by b-AP15. MelJuSo-Ub^{G76V}-YFP cells were exposed to 0.4 μM b-AP15 for 1 h, followed by medium change and incubation in drug-free medium for 0, 1, 4, 8 and 24 hours. Note that the levels of polyubiquitin conjugates decrease after removal of b-AP15 and that Ub^{G76V}-YFP and p21 levels decrease at 8 h (interpretation of 24 h time-point is difficult due to considerable cell death). Furthermore, note that caspase-3 and PARP cleavage is observed 24 h after transient drug-exposure. (C) Reversibility of proteasome inhibition by bortezomib. MelJuSo-Ub^{G76V}-YFP cells were exposed to 0.1 μM for 1 h, washed and incubated in drug-free medium. The disappearance of polyubiquitin at 24 h was not due to cell death (see Fig. 3).

Molecular Pharmacology Fast Forward. Published on April 8, 2014 as DOI: 10.1124/mol.113.091322
This article has not been copyedited and formatted. The final version may differ from this version.

Fig. 3. Commitment to apoptosis and cell death. (A) HCT116 cells were exposed to 1 μM b-AP15 or 100 nM bortezomib for different periods of time, followed by washout and incubation in drug-free medium. Apoptosis was assessed after 24 h by determination of caspase-cleaved K18 (M30 Apoptosense®). Note the short exposure times required for commitment to apoptosis by b-AP15. (B) Survival of MelJuSo cells was determined at 24 h after continuous (24 h) or transient (1 h) exposure to different concentrations of b-AP15. Viability was determined by the MTT assay (expressed as fraction between treated/control wells). (C) Survival of MelJuSo cells was determined at 24 h after continuous (24 h) or transient (1 h) exposure to different concentrations of bortezomib.

Fig. 4. Uptake of b-AP15. (A). MelJuSo cells were exposed to b-AP15 (0.8 μM) in different concentrations of fetal calf serum and viability was determined at 24 h. (B) Uptake of [^{14}C] b-AP15 (4 μM) was determined using LigandTracer® White. Association of radioactive drug with cells was determined in real-time as described (Wang and Albertioni, 2010). Red (lower) curve: cells were pre-treated with 10 μM N-ethylmaleimide for 30 min prior to addition of [^{14}C]b-AP15 (4 μM). (**C**) Polyubiquitin conjugates do not disappear after transient exposure to higher b-AP15 concentrations. MelJuSo Ub^{G76V}-YFP cells were exposed for 1 h to the indicated concentrations of b-AP15 and either directly processed for western blot analysis (0 h) or incubated in drug-free medium for 8 h. Note that of polyubiquitin signals decrease between 0 and 8 hours after exposure to 0.4 μM and 0.6 μM b-AP15, but remain at higher concentrations.

Molecular Pharmacology Fast Forward. Published on April 8, 2014 as DOI: 10.1124/mol.113.091322
This article has not been copyedited and formatted. The final version may differ from this version.

Fig. 5. Pharmacokinetics and hepatocyte metabolism of b-AP15. (A) b-AP15 was injected into NMRI mice (3 mg/kg). Plasma was collected after different times and b-AP15 levels were determined by mass spectrometry. The earliest time-point feasible for plasma collection was 2 min; the C_0 value of 400 nM is an estimation. (B) Metabolites of b-AP15 formed in human and mouse hepatocytes. The relative quantities of the various metabolites formed during 3 h incubation are shown in Table 1.

Fig. 6. Induction of Hmox-1 by b-AP15 analogues does not correlate to polyubiquitin accumulation or induction of apoptosis. (A) MelJuSo Ub^{G76V}-YFP cells were exposed to the indicated compounds and concentrations (all in μM) for 18 h and processed for western blotting. Note that Hmox-1 expression is induced by various compound at concentrations which do not induce polyubiquitin accumulation or caspase-3 cleavage. (B) Determination of apoptosis induction using APO-BrdU™ TUNEL Assay. MelJuSo cells were exposed to vehicle (DMSO), b-AP15, b-AP107, VLX1545, VLX1547 (all at 1.5 μM) or b-AP113, VLX1550 (20μM) for 24 h. Cells were stained with Alexa Fluor® 488 dye-labeled anti-BrdU antibody and propidium iodide/RNase A and processed for flow cytometry.

Molecular Pharmacology Fast Forward. Published on April 8, 2014 as DOI: 10.1124/mol.113.091322
This article has not been copyedited and formatted. The final version may differ from this version.

Fig. 7. Inhibition of TrxR by b-AP15 can not explain apoptosis induction or proteasome inhibition. (A) TrxR enzyme activity was determined in HCT116 cells exposed to the indicated concentrations of b-AP15 for 3 h. (B) TrxR and GR enzyme activity was determined in the presence of the indicated compounds. Note that b-AP15 and its analogues inhibit TrxR (diamonds), but not GR (squares), enzyme activity. (C) Irreversible inhibition of TrxR by b-AP15. b-AP15 was added to purified TrxR and enzyme activity was determined before or after gel filtration. (D) Accumulation of caspase-cleaved K18 was determined in cell cultures after 14 h of exposure of HCT116 cells to auranofin (1.5 μM), bortezomib (0.1 μM) and/or b-AP15 (1 μM) as indicated. ELISA was used to determine caspase-cleaved K18. (E) Accumulation of caspase-cleaved K18 was determined in cell cultures after 14 h of exposure of HCT116-BCL2 cells to different drugs. Conditions the same as in (D). (F) Auranofin does not block proteasome function. HCT116, A549 or MelJuSo Ub^{G76V}-YFP cells were exposed to b-AP15 (1 μM) or auranofin (1.5 μM) for 6 h and extracts analysed by western blotting. Note that whereas auranofin induces strong Hmox-1 expression, accumulation of polyubiquitin and Ub-YFP is insignificant compared to b-AP15. A549 cells are known to constitutively express Nrf-2, leading to baseline Hmox-1 expression in the cell line.

Molecular Pharmacology Fast Forward. Published on April 8, 2014 as DOI: 10.1124/mol.113.091322
This article has not been copyedited and formatted. The final version may differ from this version.

Table 1. The relative LC/MS peak areas for b-AP15 and its metabolites in mouse and human hepatocytes.

	Area % mouse	Area % human
Parent	2.7	5.0
M1	0.5	3.6
M2	0.5	2.5
M3	0.2	1.3
M4	7.8	5.5
M5	11.4	4.8
M6	23.2	21.1
M7	6.5	0.4
M8	1.1	2.5
M9	10.0	2.0
M10	8.6	-
M11	6.5	-
M12	6.8	-
M13	1.3	3.7
M14	1.5	0.5
M15	2.8	-
M16	5.0	0.7
M17	3.7	0.6
M18	-	3.9
M19	-	1.6
M20	-	5.4
M21	-	11.0
M22	-	4.9
M23	-	19.2

The quantification is based in the assumption of identical LC/MS response between all compounds.

Figure 1

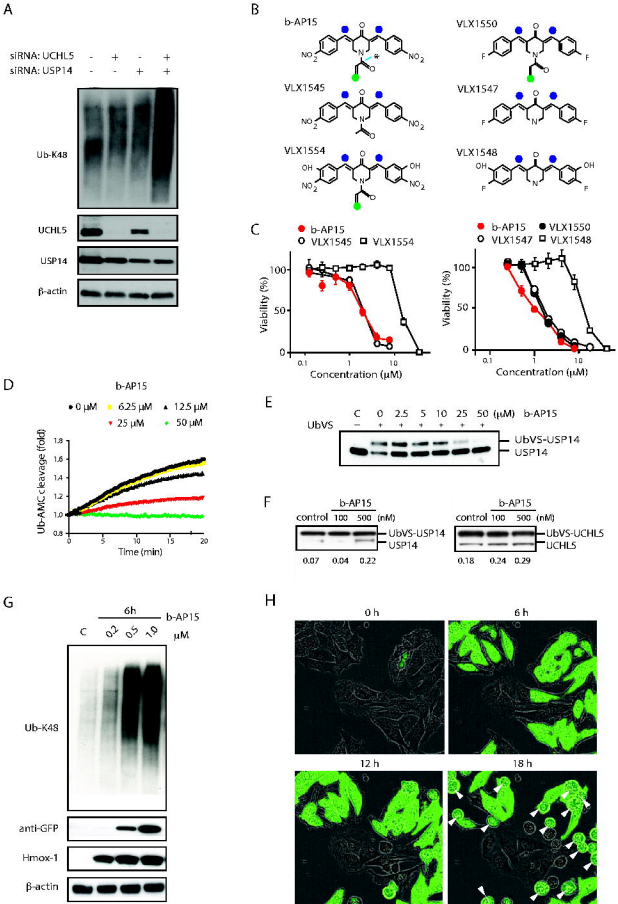
A
siRNA: UCHL5 - + - +
siRNA: USP14 - - + +
Ub-K48
UCHL5
USP14
β-actin
B
b-AP15
VLX1550
VLX1545
VLX1547
VLX1554
VLX1548
C
b-AP15
VLX1545
VLX1554
b-AP15
VLX1550
VLX1547
VLX1548
Viability (%)
Concentration (μM)
D
b-AP15
0 μM
6.25 μM
12.5 μM
25 μM
50 μM
Ub-AMC cleavage (fold)
Time (min)
E
C 0 2.5 5 10 25 50 (μM) b-AP15
UbVS
UbVS-USP14
USP14
F
b-AP15
control 100 500 (nM)
UbVS-USP14
USP14
0.07 0.04 0.22
b-AP15
control 100 500 (nM)
UbVS-UCHL5
UCHL5
0.18 0.24 0.29
G
6h
C 0.2 0.5 1.0 b-AP15 μM
Ub-K48
anti-GFP
Hmox-1
β-actin
H
0 h
6 h
12 h
18 h

Figure 2

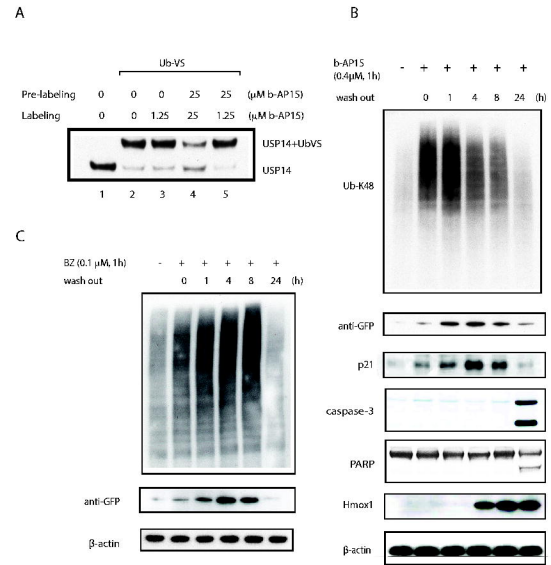
A
Ub-VS
Pre-labeling 0 0 0 25 25 (μM b-AP1S)
Labeling 0 0 1.25 25 1.25 (μM b-AP1S)
USP14+UbVS
USP14
1 2 3 4 5
B
b-AP1S (0.4μM, 1h) - + + + + +
wash out 0 1 4 8 24 (h)
Ub-K48
anti-GFP
p21
caspase-3
PARP
Hmox1
β-actin
C
BZ (0.1 μM, 1h) - + + + + +
wash out 0 1 4 8 24 (h)
anti-GFP
β-actin

Figure 3

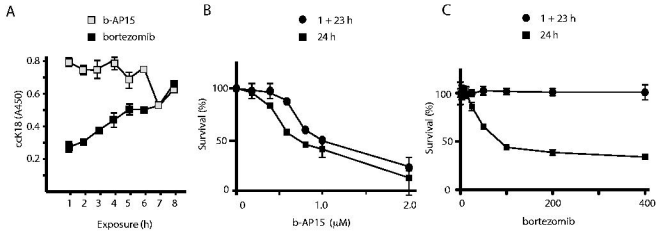
A
b-AP15
bortezomib
ccK18 (A450)
0.8
0.6
0.4
0.2
1 2 3 4 5 6 7 8
Exposure (h)
B
1 + 23 h
24 h
Survival (%)
100
50
0
0
1.0
2.0
b-AP15 (μM)
C
1 + 23 h
24 h
Survival (%)
100
50
0
0
200
400
bortezomib

Figure 4

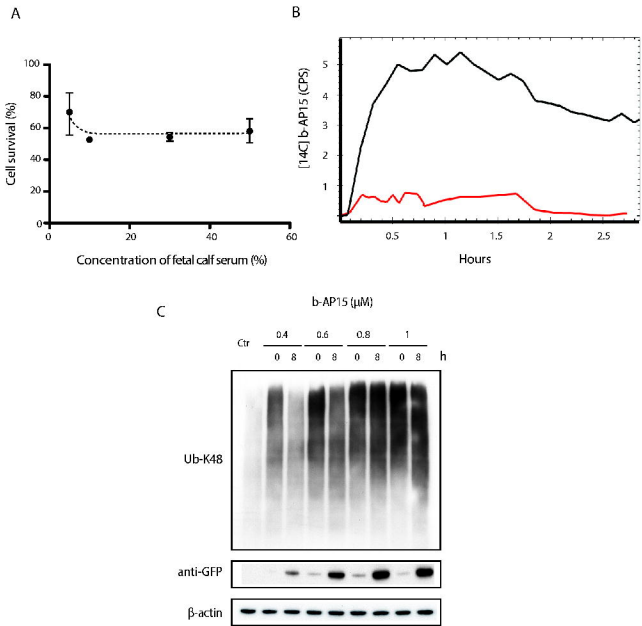
A
Cell survival (%)
100
80
60
40
20
0
0
20
40
60
Concentration of fetal calf serum (%)
B
[14C] b-AP15 (CPS)
5
4
3
2
1
0.5
1
1.5
2
2.5
Hours
C
b-AP15 (μM)
Ctr
0.4
0.6
0.8
1
0 8 0 8 0 8 0 8 h
Ub-K48
anti-GFP
β-actin

FIGURE 5

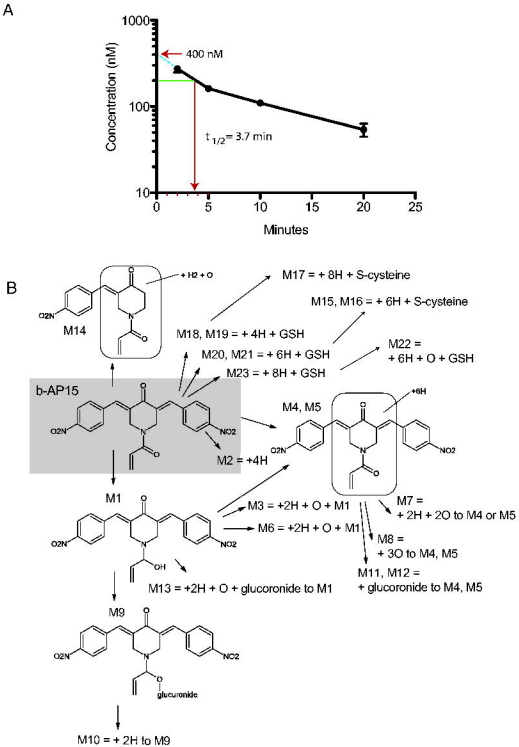
A
1000
400 nM
Concentration (nM)
100
$t_{1/2}$= 3.7 min
10
0
5
10
15
20
25
Minutes
B
M14
+ H2 + O
M17 = + 8H + S-cysteine
M15, M16 = + 6H + S-cysteine
M18, M19 = + 4H + GSH
M20, M21 = + 6H + GSH
M22 = + 6H + O + GSH
M23 = + 8H + GSH
b-AP15
M4, M5
+6H
M2 = +4H
M1
M3 = +2H + O + M1
M7 = + 2H + 2O to M4 or M5
M6 = +2H + O + M1
M8 = + 3O to M4, M5
M11, M12 = + glucoronide to M4, M5
M13 = +2H + O + glucoronide to M1
M9
glucuronide
M10 = + 2H to M9

Figure 6

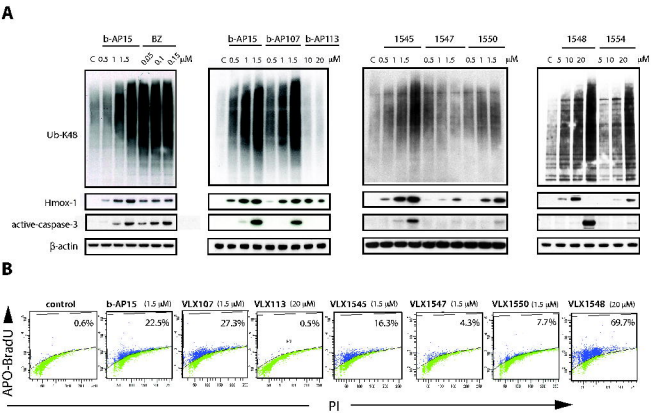
A
b-AP15
BZ
C 0.5 1 1.5 0.025 0.1 0.15 μM
b-AP15
b-AP107
b-AP113
C 0.5 1 1.5 0.5 1 1.5 10 20 μM
1545
1547
1550
C 0.5 1 1.5 0.3 1 1.5 0.5 1 1.5 μM
1548
1554
C 5 10 20 5 10 20 uM
Ub-K48
Hmox-1
active-caspase-3
β-actin
B
control
b-AP15 (1.5 μM)
VLX107 (1.5 μM)
VLX113 (20 μM)
VLX1545 (1.5 μM)
VLX1547 (1.5 μM)
VLX1550 (1.5 μM)
VLX1548 (20 μM)
0.6%
22.5%
27.3%
0.5%
16.3%
4.3%
7.7%
69.7%
APO-BradU
PI

Figure 7

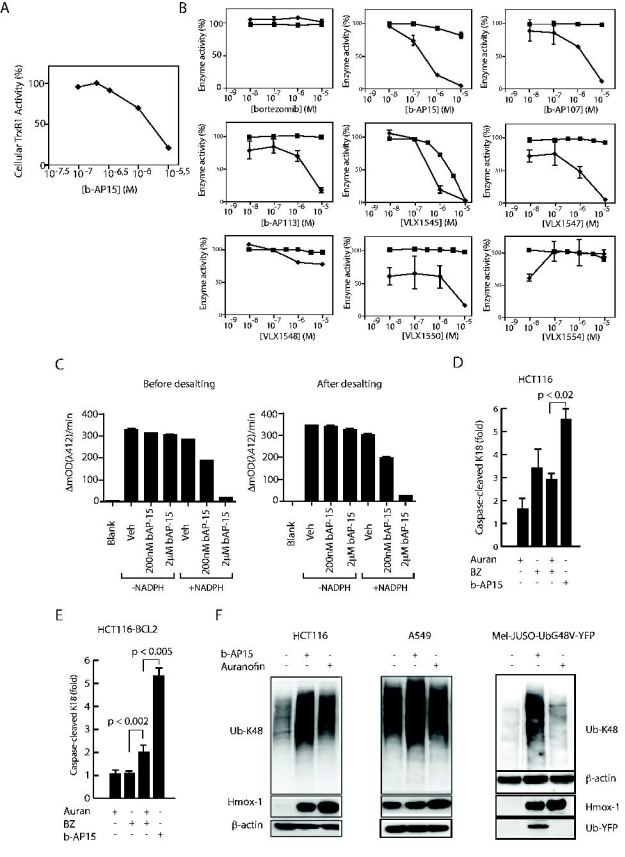
A
Cellular TrxR1 Activity (%)
[b-AP15] (M)
B
Enzyme activity (%)
[bortezomib] (M)
[b-AP15] (M)
[b-AP107] (M)
[b-AP113] (M)
[VLX1545] (M)
[VLX1547] (M)
[VLX1548] (M)
[VLX1550] (M)
[VLX1554] (M)
C
Before desalting
After desalting
ΔmOD/Δ412/min
Blank
Veh
200nM bAP-15
2μM bAP-15
-NADPH
+NADPH
D
HCT116
p < 0.02
Caspase-cleaved K18 (fold)
Auran
BZ
b-AP15
E
HCT116-BCL2
p < 0.005
p < 0.002
Caspase-cleaved K18 (fold)
F
HCT116
A549
Mel-JUSO-UbG48V-YFP
b-AP15
Auranofin
Ub-K48
Hmox-1
β-actin
Ub-YFP